Conf-920308--12

To be Presented at The American Nuclear Society Meeting,
Advances in Reactor Physics, Charleston, SC March 8-11, 1992

An Evaluation of Multigroup Flux Predictions
in the EBR-II Core

ANL/CP--73771

DE92 007379

R. N. Hill, T. H. Fanning*, and P. J. Finck

Reactor Analysis Division
Argonne National Laboratory
9700 South Cass Avenue
Argonne, IL 60439
(708) 972-4865

*Permanent Address:
Dept. of Nuclear Engineering and Engineering Physics
University of Wisconsin, Madison

Received OSTI

FEB 1 4 1992

The submitted manuscript has been authored by a contractor of the U. S. Government under contract No. W-31-109-ENG-38. Accordingly, the U. S. Government retains a nonexclusive, royalty-free license to publish or reproduce the published form of this contribution, or allow others to do so, for U. S. Government purposes.

AN EVALUATION OF MULTIGROUP FLUX PREDICTIONS IN THE EBR-II CORE

R. N. Hill, T. H. Fanning*, and P. J. Finck
Argonne National Laboratory
9700 S. Cass Ave.
Argonne, Illinois 60349-4842 USA

*Permanent Address:
Dept. of Nuclear Engineering and Engineering Physics
University of Wisconsin, Madison

ABSTRACT

The unique physics characteristics of EBR-II which are difficult to model with conventional neutronic methodologies are identified; the high neutron leakage fraction and importance of neutron reflection cause errors when conventional calculational approximations are utilizea In this paper, various conventional and higher-order group constant evaluations and flux computation methods are compared for a simplified R-Z model of the EBR-II system. Although conventional methods do provide adequate predictions of the flux in the core region, significant mispredictions are observed in the reflector and radial blanket regions. Calculational comparisons indicate that a fine energy group structure is required for accurate predictions of the eigenvalue and flux distribution; greater detail is needed in the iron resonance scattering treatment. Calculational comparisons also indicate that transport theory with detailed anisotropic scattering treatment is required.

I. INTRODUCTION

Experimental Breeder Reactor No. 2 (EBR-II) and its adjoining fuel cycle facility were originally designed and operated to provide a small plant demonstration of a sodium-cooled fast breeder power plant with an integral fuel cycle. Following successful demonstration of the plant, EBR-II has been utilized for many fast neutron irradiation and materials testing experiments. Meanwhile, significant improvements have been developed for metal fuel reprocessing; various process changes, including the use of electrorefining, have reduced the heavy metal losses from 5-10% to less than 1% and virtually eliminated the noble metals from the heavy metal product. This new reprocessing technique is the basis for the Integral Fast Reactor (IFR) fuel cycle concept. The behavior of IFR metal fuel has been investigated using irradiation experiments in EBR-II; and a key milestone of the IFR program is to demonstrate closure of the IFR fuel cycle at EBR-II.

Operation of this closed fuel cycle requires an accurate tracking of all materials during both in-core and ex-core phases. It is particularly important to trace actinide isotopes, since fissile material recovery is the primary objective in fuel reprocessing. Chemical and isotopic analyses of the discharged fuel are impractical on a large scale. Therefore, accurate core depletion calculations are necessary to specify the material composition of the spent fuel.

Methodological improvements for depletion calculations were proposed in references 1 and 2; using nodal equivalence theory, significant improvements in the depletion calculations were observed. Nodal equivalence theory provides additional degrees of freedom ("discontinuity factors") to the standard diffusion equations allowing nodal schemes to reproduce any higher order solution. For EBR-II applications, higher-order multigroup flux solutions are calculated by a series (R-Z and planar) of two-dimensional transport calculations; the results are used to create few group cross section data and a set of few group discontinuity factors. This approach allows a few-group nodal diffusion calculation (as used in the depletion computation) to account for the higher-order effects; however, any errors present in the higher-order multigroup solutions will be reproduced in the nodal solution. In this paper, the primary goal is to evaluate the accuracy of various higher-order methods for generation of EBR-II multigroup flux solutions.

Some unique physics characteristics of the EBR-II system are identified in Section II; these characteristics cause calculational difficulties which must be accounted for in accurate higher-order solutions. Many physics phenomena (i.e., axial streaming) are discussed in Section II; however, the evaluation of detailed geometric effects is beyond the scope of this paper. In this paper, the analyses focus on a simplified R-Z model of EBR-II where a minimal number of homogeneous material compositions are specified. Accurate physics predictions are difficult even in this simplified model; the high leakage probability causes a breakdown of the basic assumptions applied in many conventional neutronic methods. In this paper, EBR-II flux predictions using various methodologies for generating multigroup cross section data and for evaluating the neutron flux distribution are evaluated. The generation of group constants for EBR-II flux predictions is addressed in Section III; and different calculational methods (i.e., diffusion or transport theory) are evaluated in Section IV.

II. PHYSICS CHARACTERISTICS OF EBR-II

EBR-II is a small, sodium cooled fast reactor system with a power rating of 62.5 MWt. A simplified R-Z model of the reactor is shown in Figure 1; in the simplified model, only eight distinct material regions are specified. The core is composed of high enrichment (~70% U-235) U-10% Zr metal fuel; the reflector and grid regions are composed primarily of stainless steel. The blanket region is composed of thick metal fuel pins which contain about 0.05% Pu-239 from prior burnup. As shown in Fig. 1, the core height is ~35 cm with a core radius of 35 cm; thus, the H/D ratio is ~1/2 indicating a pancaked core geometry. Both the small core size and geometric spoiling lead to a high neutron leakage fraction; about 60% of the neutrons produced leak out of the core. The high neutron leakage fraction leads to the large discrepancies between diffusion and transport theory, as discussed in Section IV.

The ex-core configuration of EBR-II creates additional physics complications. First, in the axial direction there is a plenum region above the core and a reflector below the core (note that the pancaked design makes axial leakage dominant in the core). This leads to an axial power tilt toward the lower portion of the core. The severity of this tilt depends upon the relative importance of upper and lower leakage:

1. In the upper plenum, there is a significant streaming path within the pin which may lead to inaccuracies for a homogenized treatment.

2. In the lower reflector, there is significant reflection back into the core; this requires an accurate modeling of directional change through scattering. This treatment is further complicated by the dominance of resonance scattering in the steel reflector (see discussion below).

Thus, it is difficult to obtain accurate predictions of the axial profile even with higher-order methods.

The radial configuration of EBR-II is particularly unique. As shown in Fig. 1, the radial reflector is adjacent to the core and is surrounded by several rows of radial blanket; in conventional designs, the radial blanket is adjacent to the core and surrounded by a reflector/shield zone. Because of the high

leakage fraction, the EBR-II core relies heavily on neutron reflection to maintain criticality; thus, an accurate evaluation of the reflection rate is necessary for accurate predictions of the core multiplication factor. Prediction of neutron reflection is especially complex because the reflection involves scattering reactions which change a neutron's angle **and** energy. Radial transmission predictions are also crucial because the radial blanket assemblies produce roughly 5% of the reactor power during normal operation. Thus, accurate flux predictions in the radial blanket are essential for evaluating the local coolant outlet temperature and local fast fluence level.

Flux predictions in the ex-core regions must evaluate the transmission of neutrons through the subcritical reflector and blanket zones; physics predictions in these radial transition zones are especially difficult. As discussed in reference 3, discrepancies between predictions and experiments increase with penetration in a uniform blanket zone; in reference 4, these errors are attributed to directional effects on the transitional resonance spectra and group constants. Similar effects may occur in the iron resonances within the radial reflector; this phenomena is particularly important because resonance scattering is a principal mechanism for the reflection of neutrons back into the core. Many of the important iron resonances can be accurately modeled by refining the energy group structure; however, the narrow iron resonances and most high energy actinide resonances cannot be represented by multiple energy groups in any practical group structure.

In summary, accurate multigroup flux predictions in EBR-II are complicated by several physical phenomena. Because of the asymmetric axial profile and importance of radial transmission between the core and radial blanket, three-dimensional flux solutions are necessary. Because of errors in leakage treatment, diffusion theory is likely inadequate for this small core. In addition, a detailed energy group structure may be required for modeling the neutron reflection.

III. ANALYSIS OF GROUP CONSTANT GENERATION

As discussed above, accurate modeling of the reflection of neutrons in EBR-II may require refinements of the neutron energy group structure; because of the high leakage fraction, the core multiplication factor is particularly sensitive to the reflection rate. In addition, the prediction of radial and axial flux distributions requires an accurate modeling of the neutron transmission and reflection. To assess the importance of group structure, eigenvalue calculations for a wide variation of energy group distributions are compared.

For this analysis, fine group neutron cross sections are generated using the MC^2-2 code.[5] In MC^2-2, an infinite medium spectrum is calculated for a 2082 energy group structure with resonance reaction rates evaluated within each group using the narrow resonance approximation; combining the multigroup and resonance contributions, group constants are generated for a specified energy structure. Fine group constants were generated for three compositions (representative of the core, radial reflector, and radial blanket in EBR-II) in various energy group structures; the radial reflector group constants were also used in the plenum, grid, and axial reflector zones. The infinite medium calculation for the core composition utilized a buckling search to criticality; whereas, the reflector and blanket calculations utilized a fixed source representative of the incoming leakage source in each region.

In MC^2-2, the infinite medium spectra can be evaluated using a consistent P_1 or B_1 evaluation of the extended transport equation.[5] P_1 infinite medium calculations allow an accurate representation of the first moment of the scattering cross section; whereas, B_1 schemes account for the curvature (second moment of the flux) produced by a given buckling. Thus, P_1 group constants are more accurate when anisotropic scattering is important and B_1 calculations are preferable for high leakage cores. The two generation techniques can lead to significant differences in the transport cross section. For high leakage geometries, the transport cross sections are significantly higher for the B_1 evaluation (indicating a smaller diffusion

coefficient): however, all other group constants are virtually unchanged. Since only the transport cross section is modified, calculational differences between P_1 and B_1 group constant sets were only observed for diffusion calculations; transport theory predictions with higher-order scattering are nearly identical for the two methods.

Diffusion theory eigenvalue predictions for the P_1 and B_1 group constant sets are compared in Table I; the eigenvalues are shown for infinite medium, one-dimensional (with constant group-independent buckling), and two-dimensional calculations. As shown in Table I, large differences are observed in the infinite medium evaluations (the B_1 material buckling is 6% larger); however, these differences decrease to 2.5% and 1.0% respectively in the one- and two-dimensional calculations. This behavior is caused by the different diffusion coefficients. The smaller diffusion coefficients in the B_1 group constant set allow fewer neutrons to leak, but also create a larger curvature. Therefore, when the $D\nabla^2\phi$ leakage term is evaluated, the differences between the P_1 and B_1 sets tend to compensate. Conversely, the leakage term is DB^2 when a fixed buckling is applied; and the B_1 set allows significantly less leakage because the curvature difference is not modeled. The ~1.0% eigenvalue increase observed using B_1 group constants does not compensate for the large errors in diffusion predictions which are shown in Section IV; and the diffusion core flux predictions are observed to be more accurate for the smaller curvature P_1 group constants (see Section IV).

The effect of group structure on transport calculation eigenvalue predictions was evaluated by comparing the flux calculation predictions for a wide range of energy detail. As a starting point, consistent P_1 infinite medium calculations were utilized to generate 230 energy group constants for the core, reflector, and blanket. Using the transport theory code $TWODANT$[6], the flux distribution (S_8P_1) was calculated for the simplified R-Z model of EBR-II shown in Fig. 1. Using the 230 group R-Z flux solution, the fine energy group constants were then collapsed in detailed spatial zones. Nine, 21, 50, and 68 energy group constants were calculated for 225 spatial zones; the collapsing mesh utilized 15 axial regions (including 5 core zones) and 15 radial regions (including 7 core zones).

In Table II, the computed eigenvalues for the various group constant sets are compared to a continuous energy Monte Carlo solution (generated using the ViM[7] code); note that the VIM and MC^2-2 cross section libraries are both generated from ENDF/B-V. As shown in Table I, the eigenvalue varies by 1% Δk between 9 group and 230 group solutions; the difference decreases to 0.2% Δk if 68 energy groups are used. However, the 230 group solution is 0.9% Δk higher than the continuous energy VIM solution. Thus, several additional refinements to the group constant generation method were also investigated. Because of the "resonance-like" structure of the iron scattering cross section above the resolved resonance range, important self-shielding effects may be neglected in the conventional 2082 energy group MC^2-2 library. As shown in Table II, when these self-shielding effects are modeled, the eigenvalue is 0.4% Δk lower. Use of a 274 energy group structure with particular detail in the high-energy iron resonances was also analyzed. Using the 274 energy group structure and the specialized self-shielding treatment of the high-energy iron cross section, the eigenvalue decreases by another 0.3% Δk as shown in Table I.

An eigenvalue discrepancy of 0.2% Δk remains between the Monte Carlo and fine group transport solutions. Consistency between the Monte Carlo and transport evaluations was demonstrated by comparing multigroup Monte Carlo and transport predictions utilizing identical group constants; errors of less than 1σ were observed for Monte Carlo runs with a standard deviation (σ) of ~ 0.01% Δk. Thus, the remaining discrepancy is most likely caused by differences between the continuous energy and fine group structures. Ongoing analyses are investigating the consistency of the VIM and multigroup cross section libraries; preliminary results indicate that some discrepancies are still present in the evaluation of scattering cross sections in the radial reflector.

In Table II, the eigenvalue predictions for various energy group structures are evaluated; however, for core power mapping and depletion calculations, the critical parameter is the flux distribution, not the eigenvalue. In Figure 2, the total flux levels of the 9, 230, 230* (special treatment of high-energy iron cross sections), and 274* group calculations are compared for a radial traverse at the core axial mid-plane. The 9 and 230 group flux solutions are 1-2% lower than the more detailed 274* solution in the core region. However, larger differences are observed in the outer regions. The 230 group solution agrees well with the 274 group solution in the radial reflector but decreases to a 5% lower level in the outer regions of the radial blanket; smaller differences are observed for the 230* group constant set. The 9 group solution (note that the group constants are based on a spatial collapse of the 230 group solution) overpredicts the flux level in the middle of the radial reflector by 5% and then progressively underpredicts the neutron transmission leading to a 10% lower level in the outer blanket. These deviations are caused by the complex physical phenomena which complicate group condensation in these outer zones; it is difficult to accurately model the reflection and transmission in a coarse group structure.

In a similar manner, axial traverses of the 9, 230, 230*, and 274* energy group flux solutions are compared in Figure 3. Again, the flux solutions agree very well in the core region; and differences are observed in the outer regions. Errors in the 9 group solution of 5% are observed in the upper and lower reflector zones (once again the 9 group flux is higher in the reflector region); and the 230 group solutions agree well with the 274* group solution. The errors in the axial profile appear to be smaller than the radial profile differences (see Fig. 2) This behavior is likely caused by the fact that the flux level at the axial edges is attenuated by about 1 order of magnitude and at the radial edge by about 2 orders of magnitude (as compared to the core center); thus, the radial transmission problem is more severe.

In summary, it appears that accurate prediction of the eigenvalue requires a very fine energy group structure with a detailed treatment of self-shielding effects in iron; with a tailored 274 energy group structure, differences of 0.2% Δk are still observed between continuous energy and multigroup solutions. For practical applications, few-group structures are obviously desirable. Thus, methods for reducing the number of energy groups while retaining computational accuracy (i.e., specialized group structures) must be developed. In addition, the application of nodal equivalence theory to account for group condensation errors is a promising alternative.

IV. ANALYSIS OF FLUX COMPUTATION METHODS

Given a set of multigroup cross sections, various methods can be used to compute the flux distribution. Because of the high neutron leakage fraction in EBR-II, large discrepancies between diffusion and transport theory calculations are expected. Since diffusion theory tends to overpredict the neutron leakage, large underpredictions of the eigenvalue and significant errors in the radial and axial profiles can be expected.

In this paper, the accuracy of diffusion theory and various approximations in discrete ordinates transport theory are compared by analyzing flux prediction in the simplified R-Z model. Using the spatially collapsed nine group cross sections described in Section III, neutron flux calculations for the simplified R-Z model of the EBR-II core (see Fig. 1) were performed using the DIF3D [8] diffusion theory code and the TWODANT [6] transport theory code. The eigenvalue predictions are compared in Table III. Each calculation in Table III utilized an identical spatial mesh; spatial mesh convergence was verified for the S_8 solution. As expected, the transport eigenvalue is significantly (5.5% Δk) higher than the diffusion eigenvalue; thus, the transport effects are very significant for the small EBR-II core. The anisotropic scattering treatment is also observed to be crucial. The $S_4 P_0$ result is about 9% Δk too high, and the transport-corrected $S_4 P_0$ (in which the transport solution uses the transport cross section instead of the total cross section) eigenvalue is 2.5% Δk below the $S_{16} P_1$ solution. Low levels of angular quadrature appear to be sufficient; the $S_4 P_1$ eigenvalue is only 0.3% Δk too high and the $S_8 P_1$ value is within 0.05% Δk of the $S_{16} P_1$ result.

In Table III, the eigenvalue predictions for various flux calculation methods are evaluated; however, for core power mapping and depletion calculations, the critical parameter is the flux distribution, not the eigenvalue. Thus, the total flux levels of the diffusion, $S_4P_0^*$, S_8P_1, and $S_{16}P_1$ calculations are compared in Figure 4 for a radial traverse at the core axial midplane. The diffusion and transport results agree well (within 2% for total flux) in the core; however, significant deviations (up to 15%) are observed in the radial blanket. Note that the B_1 group constants described in Section III generate more curvature in the core flux distribution and lead to larger errors in the diffusion flux prediction at the core center. The diffusion calculation overpredicts the neutron leakage from the core (giving the lower eigenvalue result shown in Table III) and this causes overpredictions of the flux level which steadily increase in the outer regions. The diffusion calculation will significantly overpredict (>10%) the power and fluence levels in the radial blanket. Because the diffusion solution gives adequate predictions of the flux in the core region, critical safety parameters and depletion effects can be calculated with reasonable accuracy utilizing conventional diffusion methods; however, transport solutions are obviously necessary for accurate predictions in the radial reflector and blanket zones. The transport-corrected S_4P_0 solution also exhibits significant errors in calculated flux distribution; as shown in Fig. 4, the computed total fluxes are 3% too high at the core center, 5% too low in the radial reflector, and increase to 10% too high in the radial blanket (as compared to the $S_{16}P_1$ solution). The S_8P_1 solution agrees well with the more detailed $S_{16}P_1$ solution throughout.

A comparison of the axial flux profiles for the diffusion, $S_4P_0^*$, S_8P_1, and $S_{16}P_1$ calculations is shown in Fig. 5. As discussed in Section II, the axial flux is tilted toward the lower core because of the unequal axial reflection (plenum above the core and reflector below). The differences in total flux indicate that the axial tilt is more severe in the diffusion prediction; the B_1 group constants described in Section III would further magnify the axial tilt in the diffusion calculation by increasing the flux curvature. As discussed in Section III, the flux attenuation is less severe in the axial direction of this model; thus, smaller overpredictions are observed for the diffusion evaluation in the outer axial regions. The $S_4P_0^*$ results show similar trends to the radial comparison (see Fig. 4); the flux is underpredicted in reflector zones and overpredicted in the core (as compared to the $S_{16}P_1$ solution). Once again, the S_8P_1 solution agrees well with the reference solution.

The comparison of transport solutions indicates that simplified anisotropic scattering treatment (the $S_4P_0^*$ results) create significant errors in the eigenvalue and flux solutions. Therefore, the effect of higher-order Legendre expansions was evaluated. Since the accuracy of higher-order Legendre cross sections generated with the MC^2-2/SDX package has not been validated, higher-order Legendre scattering matrices were generated using the continuous energy VIM code.[7] For a two-region reflected sphere (with a core volume similar to EBR-II), P_5 scattering matrices were generated in the core and reflector regions; to give reasonable statistical accuracy in the individual group constant values, a coarse 9 group structure is utilized. The calculated eigenvalues for P_0 through P_5 scattering expansions are summarized in Table IV. Similar to the R-Z results a 10% eigenvalue difference is observed between eigenvalue predictions utilizing P_0 and P_1 scattering expansions; the P_0 results grossly overpredict the multiplication factor. For the P_0 evaluation, all scattering reactions lead to an isotropic outgoing neutron distribution. However, the angular flux distribution in the ex-core regions will be tilted away from the core because of the dominance of core leakage; for scattering reactions with an anisotropic scattering treatment the outgoing neutrons will tend to maintain this angular bias. Therefore, the P_0 treatment overpredicts the reflection rate. The results in Table IV also indicate a 0.4% Δk difference between P_1 and P_3 predictions; a higher eigenvalue is calculated when higher-order scattering matrices are utilized. The P_3 through P_5 eigenvalue predictions are virtually identical; thus, P_3 scattering expansions appear to be adequate in this calculation. It is important to recognize that the errors incurred in anisotropic scattering treatment may vary for different group structures; if finer group structure are utilized, the anisotropic scattering effects must be evaluated for the detailed energy structure.

In summary, large eigenvalue discrepancies (~5.5% Δk) are observed between diffusion and transport theory predictions. Although diffusion theory does provide adequate predictions of the flux level in

the core region, large discrepancies (up to 15%) are observed in the flux predictions for the reflector and blanket regions. Simplified anisotropic scattering treatments can cause significant errors in the transport theory predictions. Transport-corrected P_0 results indicate a 2.5% Δk underprediction of the eigenvalue and 5-10% errors in the flux level. In addition, preliminary results indicate a 0.4% Δk difference between P_1 and P_3 predictions. Because of the computational complexity and expense of transport calculations with detailed anisotropic scattering treatment, the application of nodal equivalence theory to account for these effects, within the framework of a diffusion code, is a promising alternative.

V. SUMMARY AND CONCLUSIONS

Because of the unique physics characteristics of EBR-II, it is difficult to obtain accurate multigroup flux predictions. The high neutron leakage fraction and importance of neutron reflection cause errors when conventional methods are utilized. In this paper, various conventional and higher-order group constant evaluations and flux computation methods are compared for a simplified R-Z model of the EBR-II system. Although conventional methods (diffusion theory with coarse group structure) do provide adequate predictions of the flux in the core region, discrepancies are observed in the reflector and radial blanket regions. Thus, to achieve accurate predictions in the outer zones, transport effects must be modeled (discrete ordinates solution or nodal equivalence diffusion solution).

Flux predictions for energy group structures ranging from 9 to 274 energy groups were evaluated. Group structures with particular detail in the high-energy iron resonance range yield superior results. Some discrepancies between continuous-energy and detailed multigroup results are still observed. Comparisons of calculational results also indicate that detailed anisotropic scattering treatment is required for accurate transport theory predictions; transport-corrected P_0 scattering matrices are clearly inferior and P_3 expansions may be required.

REFERENCES

1. P. J. Finck, R. N. Hill, and S. Sakamoto, "Improvements in EBR-II Core Depletion Calculations," Proc. Intl. Conf. on Fast Reactor and its Fuel Cycles, Kyoto, October, 1991.

2. P. J. Finck and K. L. Derstine, "The Application of Nodal Equivalence Theory to Hexagonal Geometry Lattices," Proc. Intl. Topical Mtg. on Advances in Mathematics, Computations, and Reactor Physics, Pittsburgh, April 1991.

3. R. N. Hill and K. O. Ott, "Advanced Methods Comparisons of Reaction Rates in the Purdue Fast Breeder Blanket Facility," Nuclear Science and Engineering, 103, 12 (1989).

4. R. N. Hill, K. O. Ott, and J. D. Rhodes, "Directional Effects in Transitional Resonance Spectra and Group Constants," Nuclear Science and Engineering, 103, 25 (1989).

5. H. Henryson II, B. J. Toppel, and C. G. Stenberg, "MC^2-2: A Code to Calculate Fast Neutron Spectra and Multigroup Cross Sections," ANL-8144, Argonne National Laboratory (June 1976).

6. R. E. Alcouffe, F. W. Brinkley, D. R. Marr, and R. D. O'Dell, "User's Guide for TWODANT: A Code Package for Two-Dimensional, Diffusion-Accelerated, Neutral-Particle Transport," LA-10049-M, Los Alamos National Laboratory (March 1984).

7. R. N. Blomquist, "VIM Users Guide," Applied Physics Division, Argonne National Laboratory (1987).

8. K. L. Derstine, "DIF3D: A Code to Solve One-, Two-, and Three-Dimensional Finite-Difference Diffusion Theory Problems," ANL-82-64, Argonne National Laboratory (April 1984).

Table I. Eigenvalue Comparison for P_1 and B_1 Group Constants

Model	P_1	B_1
Infinite Medium Material Buckling, B_m^2 (cm^{-2})	6.19E-3	6.55E-3
One-Dimension,[a] k_{eff}	1.0000	1.0242
Two-Dimension,[b] k_{eff}	0.9536	0.9638

[a]radial model with constant axial buckling

[b]regional depleted R-Z model

Table II. Group Structure Comparison for Simplified EBR-II R-Z Model

No. of Groups	k_{eff}
9	1.2343
21	1.2296
50	1.2282
68	1.2257
230	1.2236
230[a]	1.2195
274[a]	1.2168
VIM[b]	1.215

[a]with self-shielding of high energy iron cross sections

[b]continuous-energy Monte Carlo calculation (see Ref. 7)

Table III. Flux Method Comparison for Simplified EBR-II R-Z Model

Flux Method	k_{eff}
Diffusion	1.1782
S_4P_0	1.3218
$S_4P_0{}^a$	1.2083
S_4P_1	1.2367
S_8P_1	1.2343
$S_{12}P_1$	1.2341
$S_{16}P_1$	1.2340

[a] transport-corrected P_0

Table IV. Legendre Scattering Order Comparison for Spherical Model

Legendre Order	k_{eff}
P_0	1.2803
P_1	1.1827
P_2	1.1869
P_3	1.1867
P_4	1.1867
P_5	1.1867

All eigenvalues are calculated using S_8P_1 transport theory and nine
energy groups in a reflected sphere;
Group constants are generated using VIM (Ref. 7)
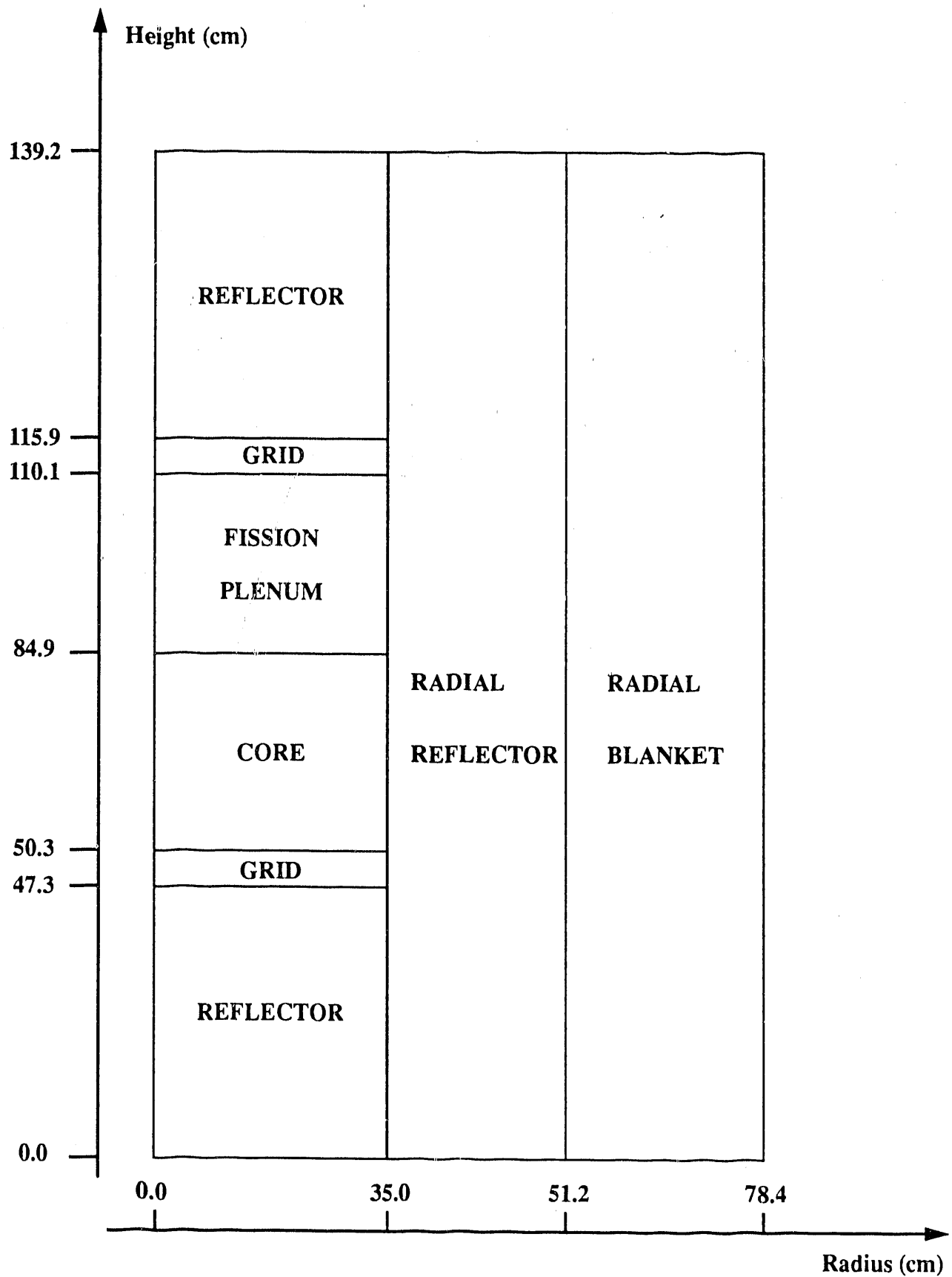
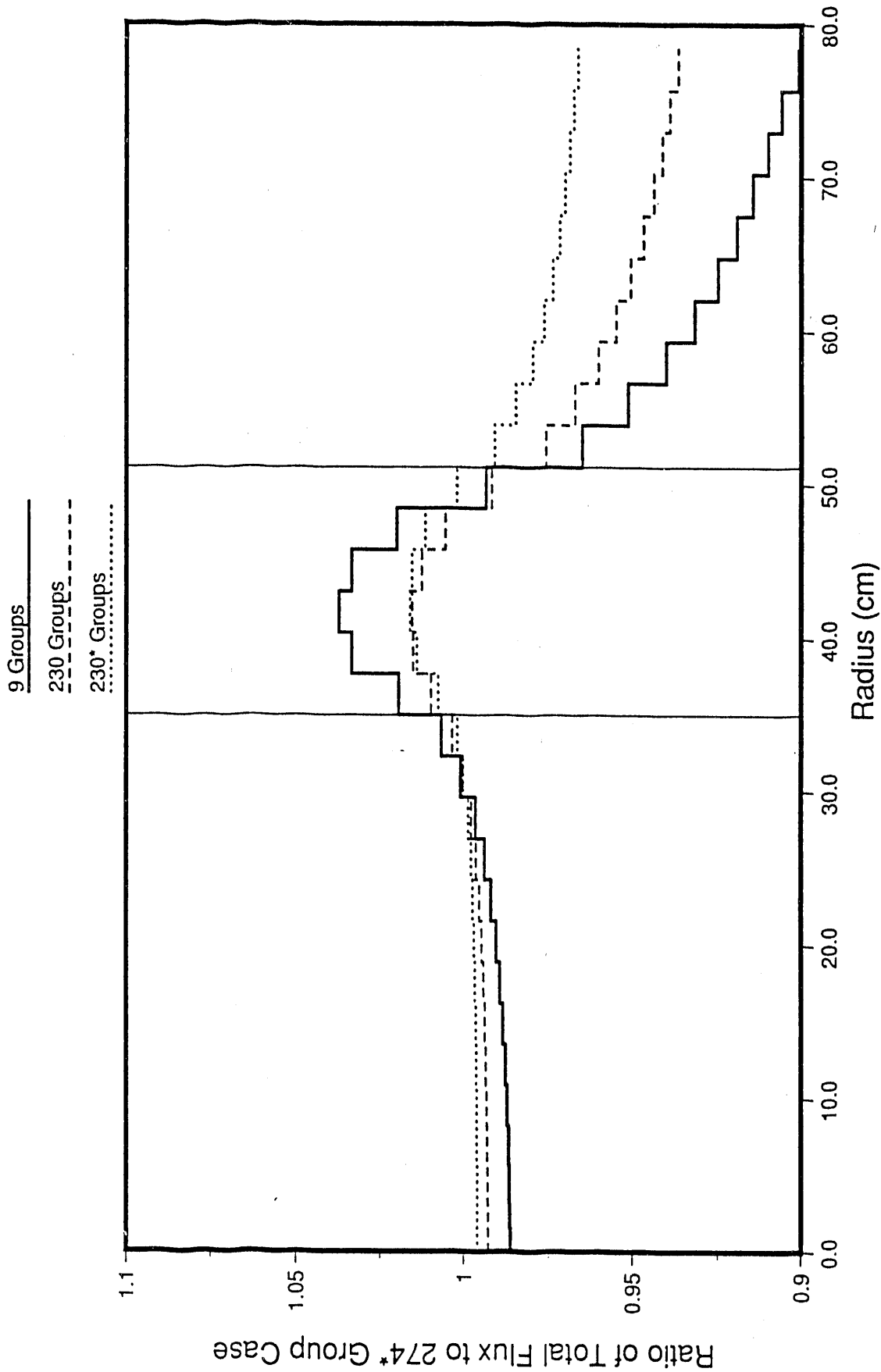Figure 1. Simplified R-Z Model of EBR-II Reactor

Figure 2.   Comparison of Total Flux Predictions using Four Different Group Structures for a Radial Traverse at the Core Axial Midplane
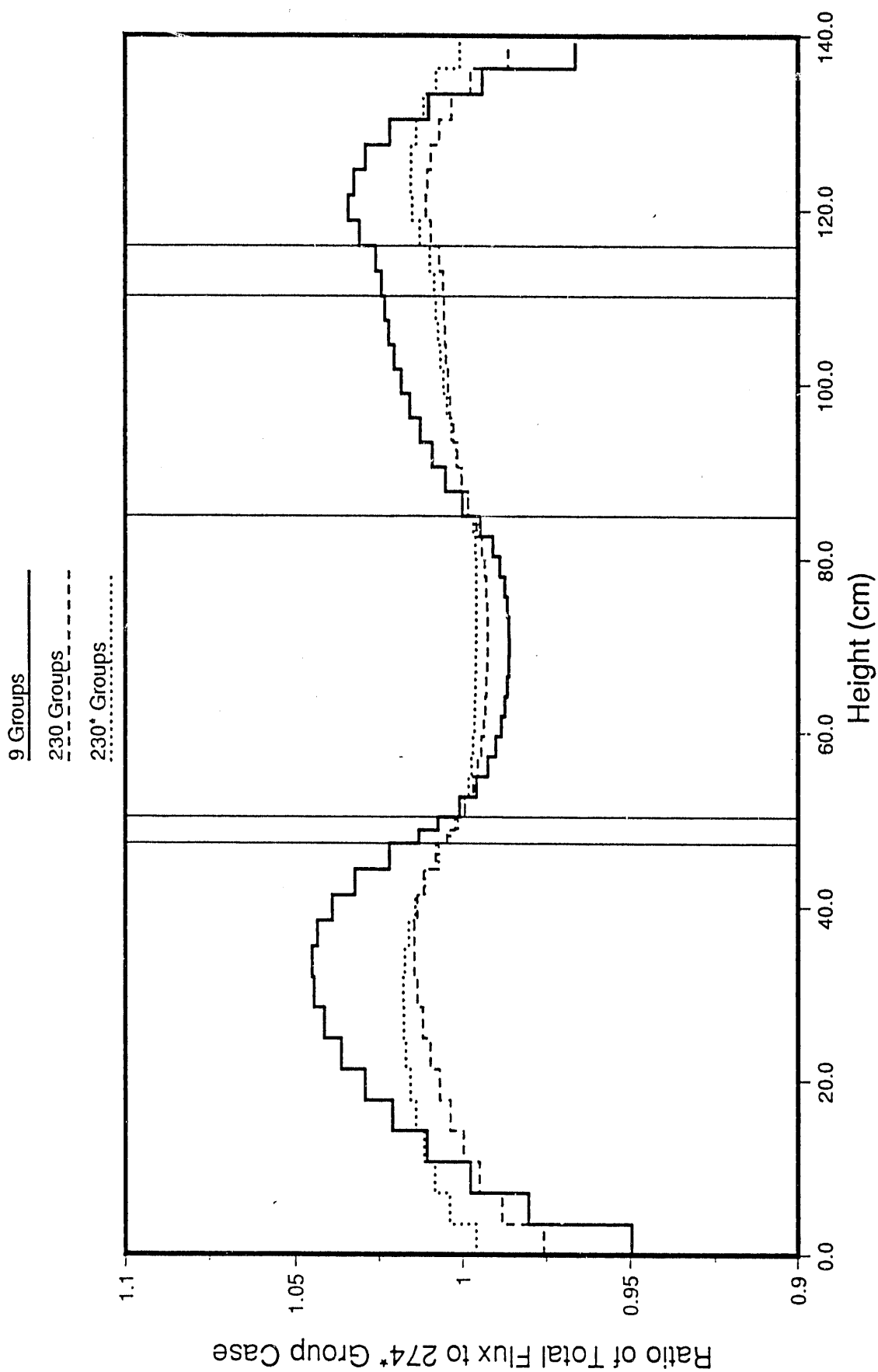
Figure 3. Comparison of Total Flux Predictions using Four Different Group Structures for an Axial Traverse at the Core Center
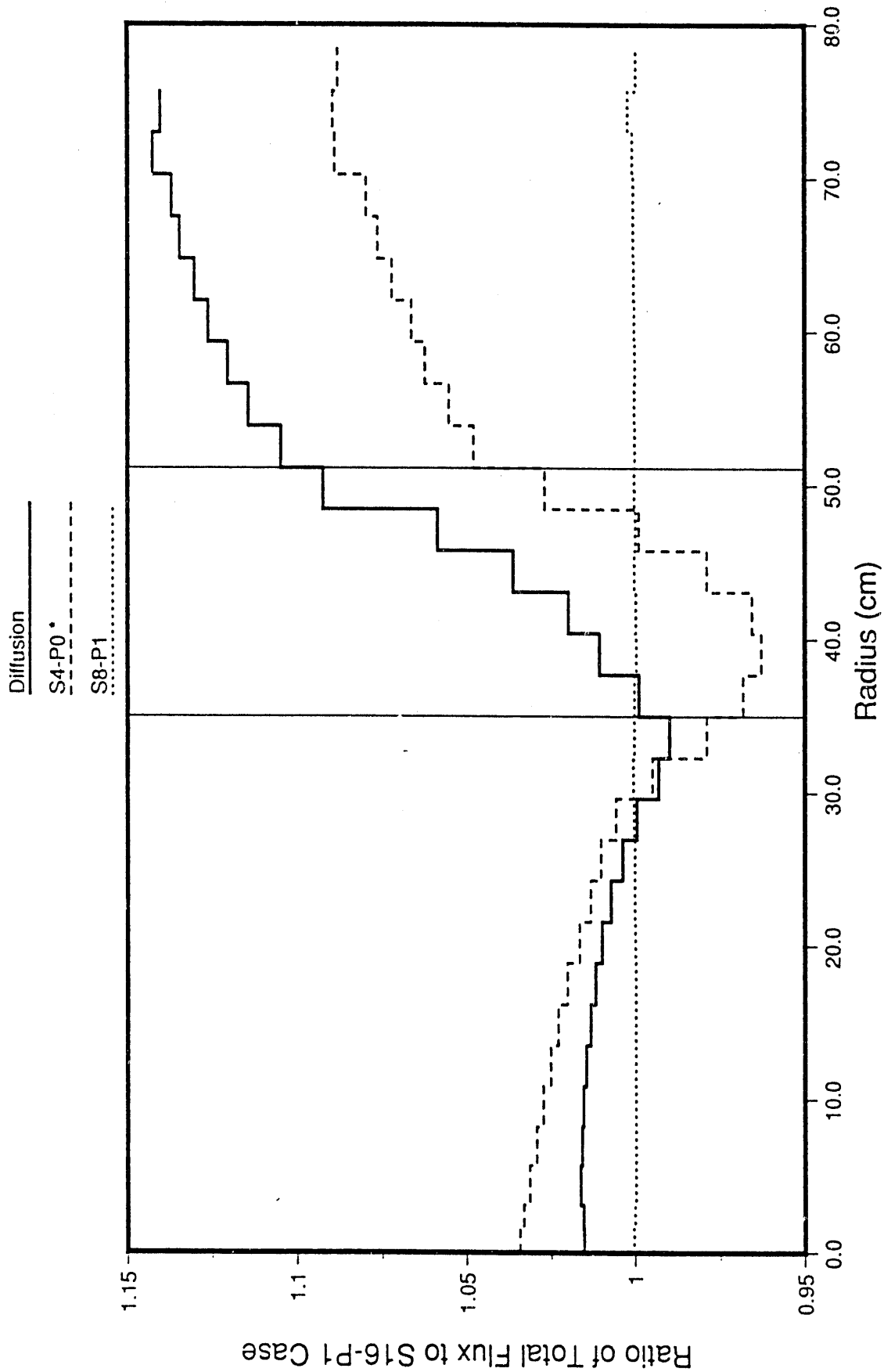
Figure 4. Comparison of Total Flux Predictions using Four Different Flux Calculation Methods for a Radial Traverse at the Core Axial Midplane
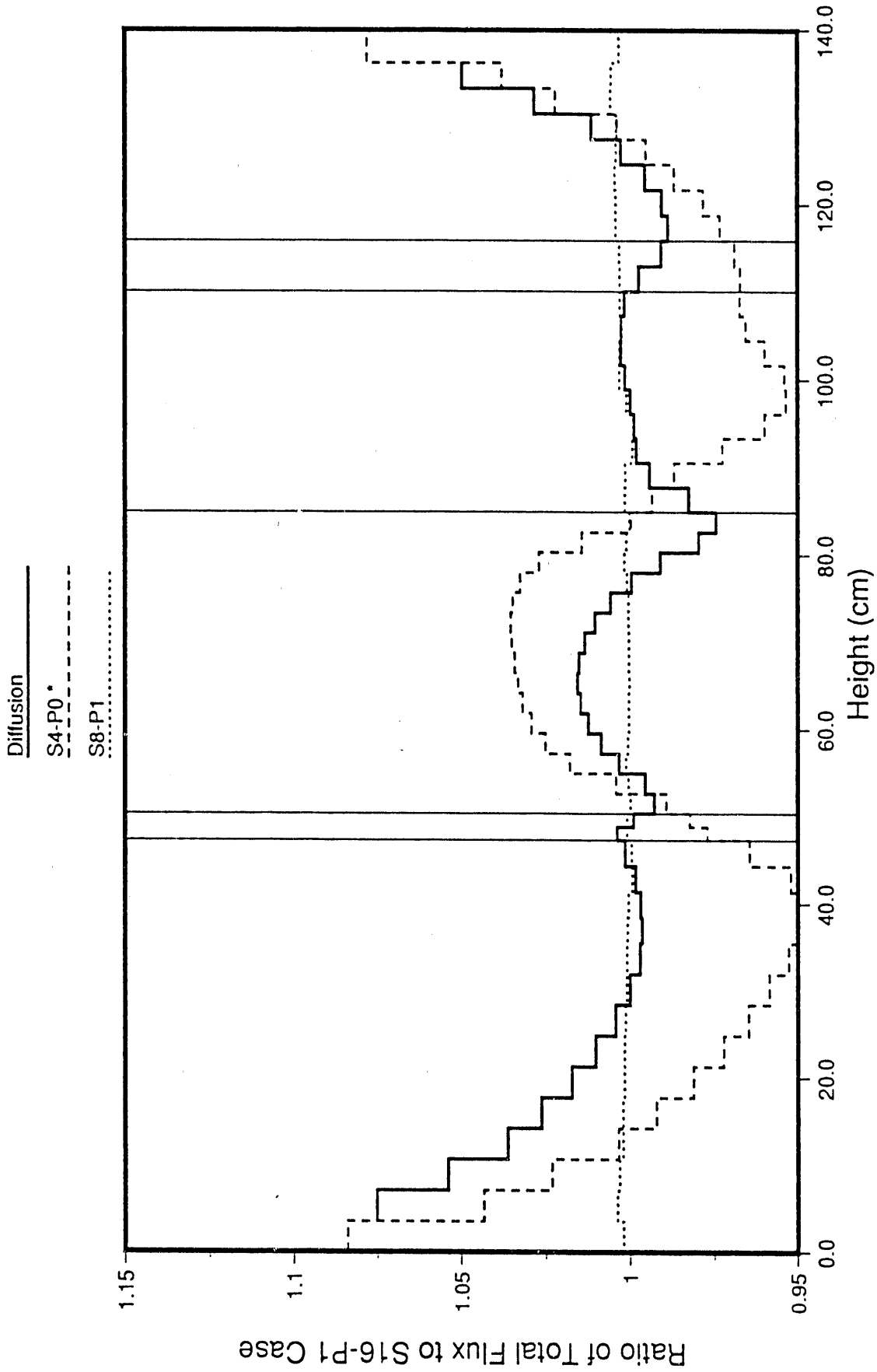
Figure 5. Comparison of Total Flux Predictions using Four Different Flux Calculation Methods for an Axial Traverse at the Core Center.

END

DATE
FILMED
3 / 11 / 92